



FFI-RAPPORT

18/00885

Non-destructive testing of graphene/ epoxy composites using Terahertz waves

Arthur D. van Rheenen
Bernt Brønmo Johnsen
Magnus W. Haakestad

Non-destructive testing of graphene/epoxy composites using Terahertz waves

Arthur D. van Rheenen
Bernt Brønmo Johnsen
Magnus W. Haakestad

Keywords

Elektromagnetiske bølger
Epoksy
Grafén
Ikke-destruktiv testing
Materialteknologi
Elektrisk ledningsevne

FFI-rapport

FFI-RAPPORT 18/00885

Prosjektnummer

504101

ISBN

P: 978-82-464-3114-7

E: 978-82-464-3115-4

Approved by

Tom Thorvaldsen, *Researcher*

Morten Huseby, *Research Manager*

Halvor Ajer, *Director of Research*

Summary

Earlier experiments have shown that composites that include carbon fibers can exhibit significant transmission of Terahertz (THz) waves, in spite of the good electrical conductivity of carbon fibers. This observation resulted in the following question: What is the relationship between the electrical conductivity and the THz-transmission of graphene/epoxy composites?

Graphene, which consists of a single layer of carbon atoms arranged in a hexagonal lattice, has attracted significant interest the last years. The unusual properties of graphene include high strength, and good conductance of electricity and heat. Mixing of graphene powder into epoxy may open up the possibility of obtaining a composite with interesting properties, for example for applications within electromagnetic shielding. Previous studies of the electrical properties of graphene/epoxy composites have been reported, but to our knowledge, Terahertz (THz) waves have not previously been used to characterize such composites.

In this study, epoxy samples with dispersed graphene powder were characterized experimentally in two different ways. In the first set of experiments, the electrical conductivity of the samples was measured. In the second set of experiments, transmission of THz waves through the samples was used to retrieve the dielectric material parameters. Finally, the measured THz transmission was compared to results from the electrical conductivity measurements. It turned out that the electrical conductivity was several orders of magnitude too low to explain the absorption of THz waves.

This study is of a more fundamental nature, but based on this material system, there can be immediate significance for military applications, such as radar absorbers. The same composite materials can also be relevant to other military applications.

Sammendrag

I tidligere eksperimenter er det observert at karbonfiber/epoksy-kompositter kan transmittere Terahertz (THz)-bølger – til tross for den gode elektriske ledningsevnen til karbonfibrene. Dette formet utgangspunktet for studien beskrevet i denne rapporten: Hva er sammenhengen mellom den elektriske ledningsevnen og transmittans i THz-frekvensområdet for kompositter laget av grafén og epoksy?

Grafén, som består av et enkelt lag av karbonatomer, har fått mye oppmerksomhet de siste åra. Noen av de uvanlige egenskapene er fantastisk styrke og god ledningsevne for både elektrisk strøm og varme. Når grafén blandes i epoksy, får man kompositter med interessante egenskaper, for eksempel skjerming for elektromagnetisk stråling. Det fins noe litteratur om materialets ledningsevne, men så vidt vi kan bedømme, er ikke THz-stråling blitt benyttet for å karakterisere komposittenes transmisjon.

Epoksyprøver med dispergert grafénpulver ble undersøkt eksperimentelt i to forskjellige oppsett. I de første eksperimentene ble den elektriske ledningsevnen til prøvene målt. I de andre eksperimentene ble transmisjon av THz-bølger gjennom prøvene brukt til å finne de dielektriske materialparameterne. Til slutt ble resultatene fra THz-målingene sammenlignet med resultatene fra ledningsevнемålingene. Det viste seg at den elektriske ledningsevnen var flere størrelsesordener for lav til å forklare den målte absorpsjonskoeffisienten for THz-strålingen.

Den rapporterte studien er av mer fundamental art, men kan umiddelbart være av betydning for grafén/epoksy-kompositter som anvendes i radarabsorbere. De samme komposittmaterialene kan også være relevante for andre militære anvendelsesområder.

Content

Summary	3
Sammendrag	4
1 Introduction	7
2 Terahertz technology	8
3 FFI's terahertz equipment	9
4 Configuration of experimental set-up	11
5 Graphene/epoxy composite samples	13
6 Electrical conductivity measurements	14
7 Terahertz measurements	16
8 Discussion	18
9 Conclusions	19
10 Future work	19
11 Acknowledgement	20
Appendix	21
References	23



1 Introduction

Graphene, which consists of a single layer of carbon atoms arranged in a hexagonal lattice, has attracted significant interest the last years. The unusual properties of graphene include high strength, and good conductance of electricity and heat. Mixing of graphene powder into epoxy may open up the possibility of obtaining a composite with interesting properties, for example for applications within electromagnetic shielding. Previous studies of the electrical properties of graphene/epoxy composites have been reported in [4-8], but to our knowledge, Terahertz (THz) waves have not previously been used to characterize such composites.

In this study, we have made graphene/epoxy composites and characterized the samples by measuring the electric conductivity and the transmission of THz waves through the samples. Dispersion of graphene powder in epoxy resin and hardener was performed by CealTech, (www.cealtech.com), and the composite samples were subsequently fabricated and characterized at FFI. One of the goals with the experiments was to investigate the possible connection between graphene concentration, electrical conductivity, and absorption. In an earlier study, carbon fibers embedded in epoxy allowed for transmission of THz radiation. This was a somewhat unexpected result because the carbon fibers are assumed to be good electrical conductors, which, in general, shield against penetration of electro-magnetic radiation.

This study was supported by the “Kompetansegruppe Materialteknologi” at FFI in an effort to explore one possible application area of graphene. A total of 150 000 kr was provided by the Kompetansedimensjon for this study, which then should cover all expenses. In this study, FFI received no-cost support from CealTech in the preparation of graphene/epoxy mixtures, which was helpful in several ways.

Other than the application studied here, graphene is considered to have a wide potential for use in military applications. On a longer term, it is expected that graphene can lead to significant improvements in materials for applications in aerospace (composite structures), high frequency electronics (terahertz, radar, cooling), functional coatings (anti-icing, corrosion protection), energy storage (batteries, ultracapacitors), camouflage (radar absorbers), weapon technologies (energetics, missiles), protection (armour, textiles), sensors (photodetectors, pressure/strain, chemical) and portable devices (displays) [9]. Beneficial effects such as improved multi-functionality, improved robustness, longer lifetime and reduced weight are expected. The importance of graphene as an emerging technology for military applications is highlighted in the AVT-304-Research Specialist’s Meeting on “Graphene technologies and applications for defence”, which is held in October 2019 in Trondheim, Norway, and organized by the Applied Vehicles Technology Panel of the Science and Technology Organization (STO) in NATO.

2 Terahertz technology

In radar technology, the frequencies have been pushed upwards, through the Gigahertz (GHz) domain up to several hundred GHz. On the other hand, the optical spectrum has been explored from the visible, through mid-IR (3-5 μm) and long-wave IR (8-12 μm) to extremely-long-wave IR ($\sim 100 \mu\text{m}$) wavelengths. Pushes from both sides have now made available both sources and detectors operating in the 0.1 – 10 THz frequency domain. In the wavelength domain, this corresponds to 3 mm – 30 μm , as shown in Figure 2.1. It was quickly recognized that many larger molecules have vibrational or rotational modes whose energies correspond to the energy of a THz photon (1 THz $\sim 4 \text{ meV}$), so that these molecules could absorb THz radiation, giving rise to absorption lines in the transmission or reflection spectrum when the molecules were exposed to broadband THz radiation. Explosives and drugs are examples of substances that have typical spectral fingerprints in the THz frequency domain. In addition, a number of common barrier materials such as paper, cardboard, plastic, and clothing are almost transparent to THz radiation. THz technology could then be used to detect and identify these substances at airport security checkpoints, or to detect hidden explosives in the military operating theatre, preferably at a safe distance [1]. In recent years, focus in the THz community has shifted to non-destructive testing (NDT) of materials. NDT refers to methods for inspection of materials or structures without permanently altering the inspected objects. NDT is important within quality control during manufacturing, but also for inspection of materials or components on a regular basis to look for damage. Examples of applications of THz technology within NDT include inspection of car paint layers and inspection of coating thickness for pharmaceutical tablets. One especially interesting application of NDT with THz waves is within analysis of composite materials [2]. This type of materials can be engineered to be both stronger and lighter than traditional materials, such as metals, and they are therefore employed in for example aircrafts, body armor, automotive components, buildings, and sports equipment.

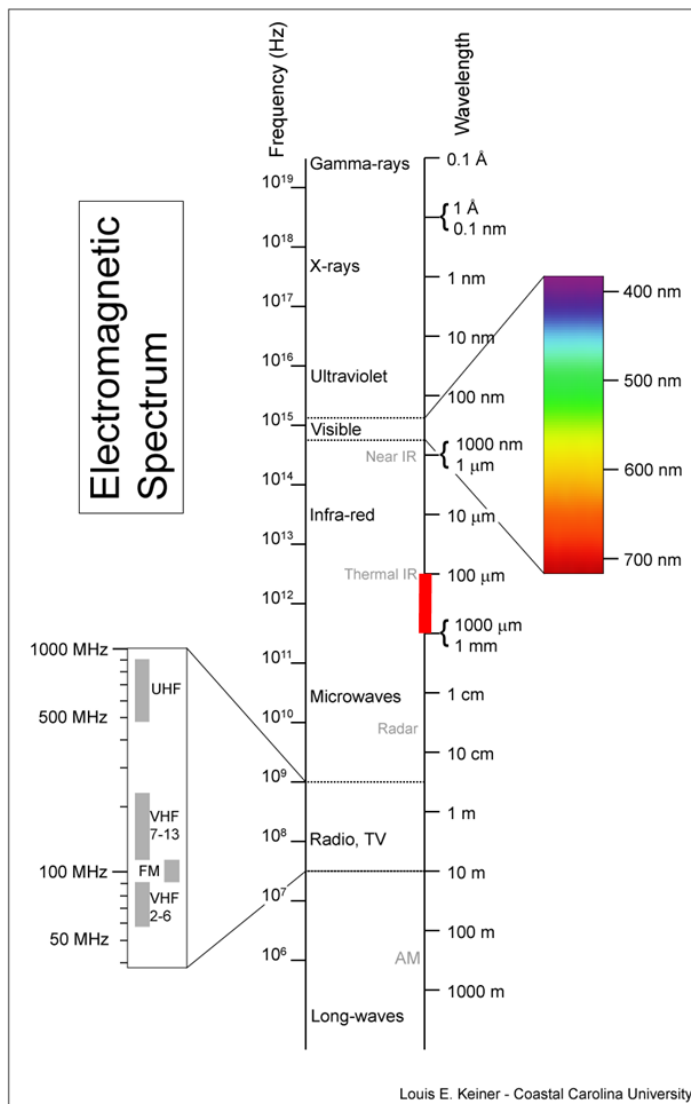


Figure 2.1 The electromagnetic spectrum with the terahertz range (0.1 mm – 1 mm wavelength) marked by a red line.

3 FFI's terahertz equipment

In August 2009, FFI purchased a time-domain spectroscopy system (THz-TDS) from Fraunhofer Institute for Physical Measurements [3]. The THz system is schematically shown in Figure 3.1. It uses a so-called femtosecond laser, a laser that emits 120 fs pulses at a wavelength of about 1.55 μm . The wavelength of the pulses is halved (frequency doubling) using a

nonlinear crystal, and these pulses then illuminate a piece of low-temperature grown GaAs where they create electron-hole pairs that are accelerated in an applied electric field and in the process emit electromagnetic radiation that mainly covers the THz frequency domain. The frequency doubling of the laser light is necessary to excite electrons above the GaAs bandgap. The advantage of the low-temperature grown material is that it has many electron and hole traps, making the carrier lifetime very short, allowing for high pulse repetition rates. The repetition rate of the laser is 90 MHz. The THz radiation is pointed to a sample and a detector measures either the reflected or transmitted THz radiation. The detection principle is the inverse of the generation principle. Part of the original laser light is diverted through a variable delay line and shone on the detector to create electron-hole pairs and prepare the detector for reception of the THz radiation. The E-field from the THz pulse then produces a tiny current in the detector, which is subsequently detected by a lock-in amplifier. One then steps through the detected pulse by adjusting the delay line and in this way builds up the transmitted or reflected THz wave. Fiber coupling of the laser light into the measurement heads allows for flexible placement of the detector end emitter with respect to the sample.

The equipment is controlled remotely from a portable PC (laptop), as is the data acquisition. A USB cable connects the PC to the controller.

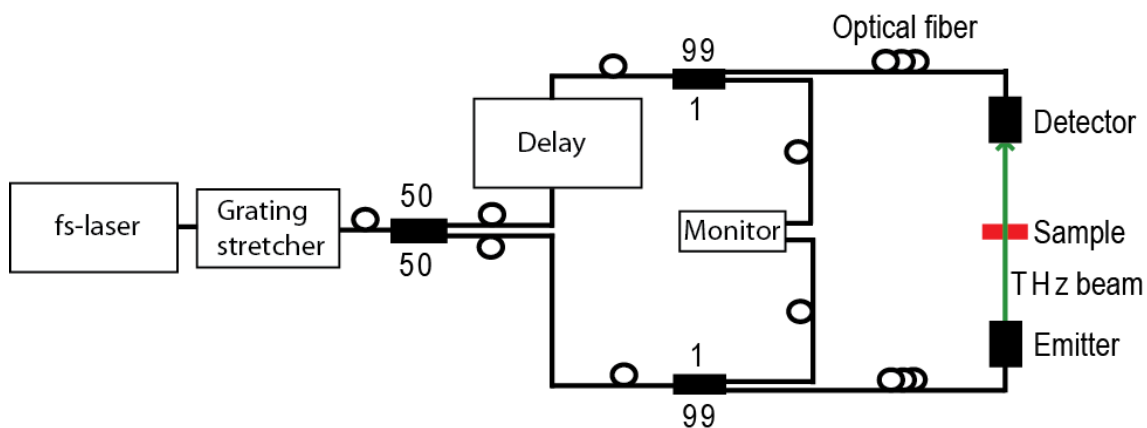


Figure 3.1 Schematic overview of FFI's fiber-coupled THz-TDS system configured in transmission mode [3].

Figure 3.2(a) shows an example of measured THz signal, in this case caused by propagation through 26 cm air. By taking the Fourier transform of the measured time domain signal, one can determine the corresponding spectrum, as shown in Figure 3.2(b). The many narrow absorption lines above 0.5 THz are caused by water vapor in air.

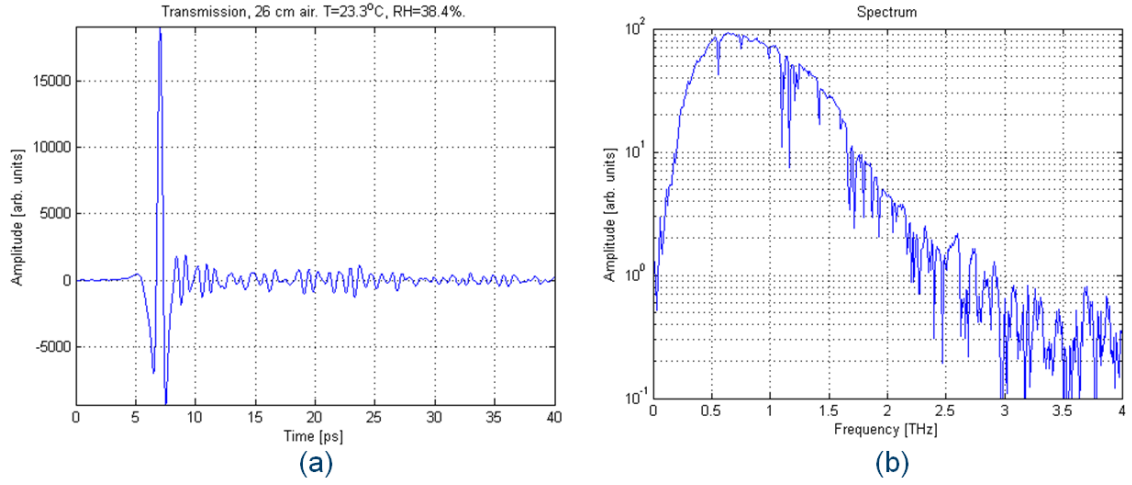


Figure 3.2 Example of measured THz-pulse after propagation through 26 cm air (a) and corresponding spectrum (b).

4 Configuration of experimental set-up

In the detection scheme used here, one uses the same laser pulse, split into two beams, to both generate and detect the THz pulse. The transmission measurements are performed by measuring the THz amplitude with and without a sample present and averaging over a large number of pulses to improve the signal-to-noise ratio. By considering the transmission of plane electromagnetic waves through a slab at normal incidence, one can derive an expression for the transmission coefficient. See Figure 4.1 for a sketch of the transmitted and reflected waves, the basis for the analysis. When neglecting multiple reflections in the sample, assuming that air has a refractive index of 1, and assuming that there are no strong absorption lines, such that the imaginary part of the index of refraction, $\text{Im } n$, is much less than the real part, $\text{Re } n$, we find that

$$\frac{E_s(\omega)}{E_r(\omega)} \approx \frac{4 \text{Re } n}{(\text{Re } n + 1)^2} \exp[i\omega(n-1)L/c] \quad (1)$$

where $E_s(\omega)$ and $E_r(\omega)$ are the Fourier transform of the measured temporal THz amplitude with and without sample, respectively. L is the sample thickness, ω is the angular frequency, and c is the vacuum speed of light. From Eq. (1), we obtain

$$\operatorname{Re} n = \frac{c}{\omega L} \operatorname{Im} \left[\ln \left(\frac{E_s(\omega)}{E_r(\omega)} \right) \right] + 1, \quad (2)$$

and

$$\operatorname{Im} n = \frac{c}{\omega L} \left\{ \ln \left[\frac{4 \operatorname{Re} n}{(\operatorname{Re} n + 1)^2} \right] - \operatorname{Re} \left[\ln \left(\frac{E_s(\omega)}{E_r(\omega)} \right) \right] \right\}. \quad (3)$$

The relation between $\operatorname{Im} n$ and the power absorption coefficient, α , is given by

$$\alpha = \frac{2\omega}{c} \operatorname{Im} n. \quad (4)$$

In essence, $\operatorname{Im} n$ denotes the absorption per wavelength, while α is the absorption per length unit. Note that $\operatorname{Im} n > 0$ for $\omega > 0$ for any passive medium, i.e. a passive medium is always lossy. A retrieved $\operatorname{Im} n < 0$ is unphysical and indicates uncertainties in the measurement results. One essential point with Eq. (3) is that it takes into account Fresnel reflection at the sample boundary, in order to get the intrinsic absorption coefficient of the sample.

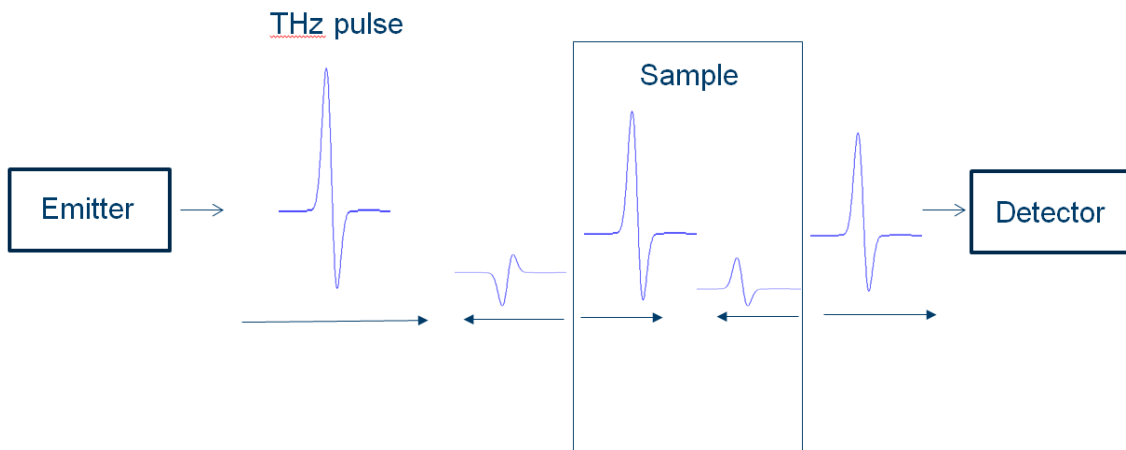


Figure 4.1 Measurement geometry for transmission mode.

5 Graphene/epoxy composite samples

Samples of neat epoxy polymer and graphene/epoxy composites were prepared. The neat epoxy sample was included as a reference.

The neat epoxy polymer samples were prepared by mixing Araldite LY 556 epoxy resin, Aradur 917 hardener, and Accelerator DY 070 at the weight ratio 100:90:1. The blend was mixed manually, heated to 60°C, and then mixed thoroughly again. The blend was then cast in aluminium cups that had been coated with a release agent. The employed curing cycle was 4 hours at 80°C and 8 hours at 140°C. The size of the cured samples was around 41 mm in diameter and 1-2 mm in thickness.

For preparation of cured graphene/epoxy samples, master batches of graphene in the epoxy resin (Araldite LY 556) or the hardener (Aradur 917), were employed. The master batches were prepared by CealTech AS using their proprietary methods to ensure stable and homogeneous dispersion at various graphene concentrations (up to 16 wt. %). A solvent-based method was employed to disperse a commercial graphene powder into the epoxy resin or hardener. The solvent helps the polymer chains to intercalate in-between the graphene sheets and exfoliate the sheets while dispersing them. The solvent was subsequently removed, leading to the formation of graphene/epoxy and graphene/hardener master batches. The master batches that were employed to prepare the graphene/epoxy samples are listed in Appendix A.1.

The graphene/epoxy samples were prepared in a similar manner to the neat epoxy samples, making sure that the mixing ratio of the polymer components was correct. However, the graphene master batches were highly viscous. To lower the viscosity during processing, they were therefore heated to 60°C prior to mixing. Using this method, graphene/epoxy samples with graphene concentration up to 12 wt. % could be fabricated. The cured samples seemed to be free of voids by visual inspection. A list of all the samples that were prepared is given in Appendix A.1, and examples of samples are shown in Figure 5.1.

The fabricated samples were subsequently characterized in terms of electrical conductivity and THz transmission.

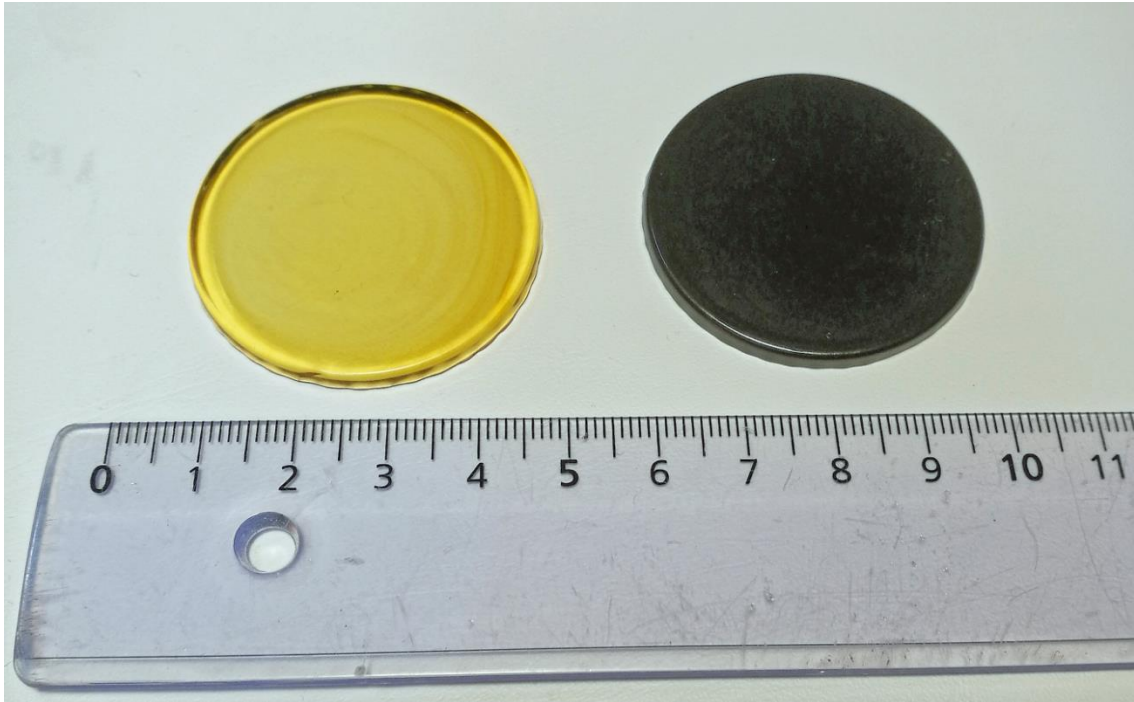


Figure 5.1 Examples of fabricated samples. Neat epoxy (left) and graphene/epoxy composite with dispersed graphene powder (right).

6 Electrical conductivity measurements

One characteristic of the samples is the electrical conductivity, which relates the current density through the sample to an applied electric field. The current density is related to the electric field according to the relation

$$\vec{j} = \sigma \vec{E}, \quad (5)$$

where \vec{j} is the electrical current density \vec{E} is the electric field and σ is the electrical conductivity. The electrical conductivity of the samples was determined using the measurement geometry in Figure 6.1. Let A be the area of each electrode in contact with the sample and d be the sample thickness. The total current passing through the sample is $I \approx jA$ and the potential difference between the electrodes is $V \approx Ed$. From Eq. (5) we then obtain

$$\sigma \approx \frac{d I}{A V}. \quad (6)$$

Thus, by applying a voltage V between the electrodes and measuring the current passing through the samples, we can determine the electrical conductivity.

Figure 6.2 shows the measured electrical conductivity as a function of graphene concentration for the different samples, which are listed in Appendix A.1. We observe that the conductivity is of the order of 10^{-12} S/m for the lowest graphene concentrations, while it increases to 10^{-5} S/m for the highest graphene concentration. The latter is still a low conductivity, and it corresponds to a measured resistance of about 100 k Ω through the sample. We further observe that there is good correspondence between graphene concentration and conductivity, except for the samples prepared from the master batch with 16 wt. % graphene in hardener.

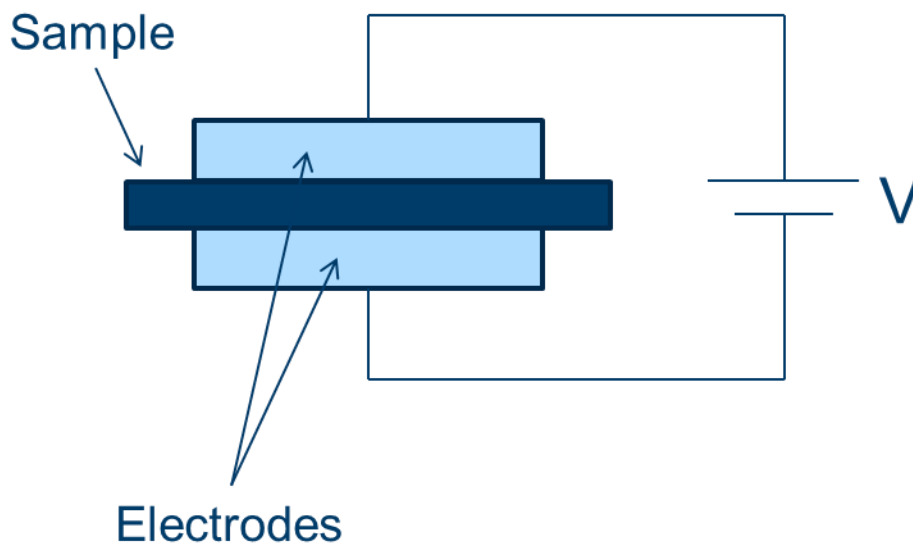


Figure 6.1 Setup for measurement of electrical conductivity. The sample to be tested is placed between two electrodes, which are pressed onto the sample using a vise. The current through the sample is measured as a function of applied voltage.

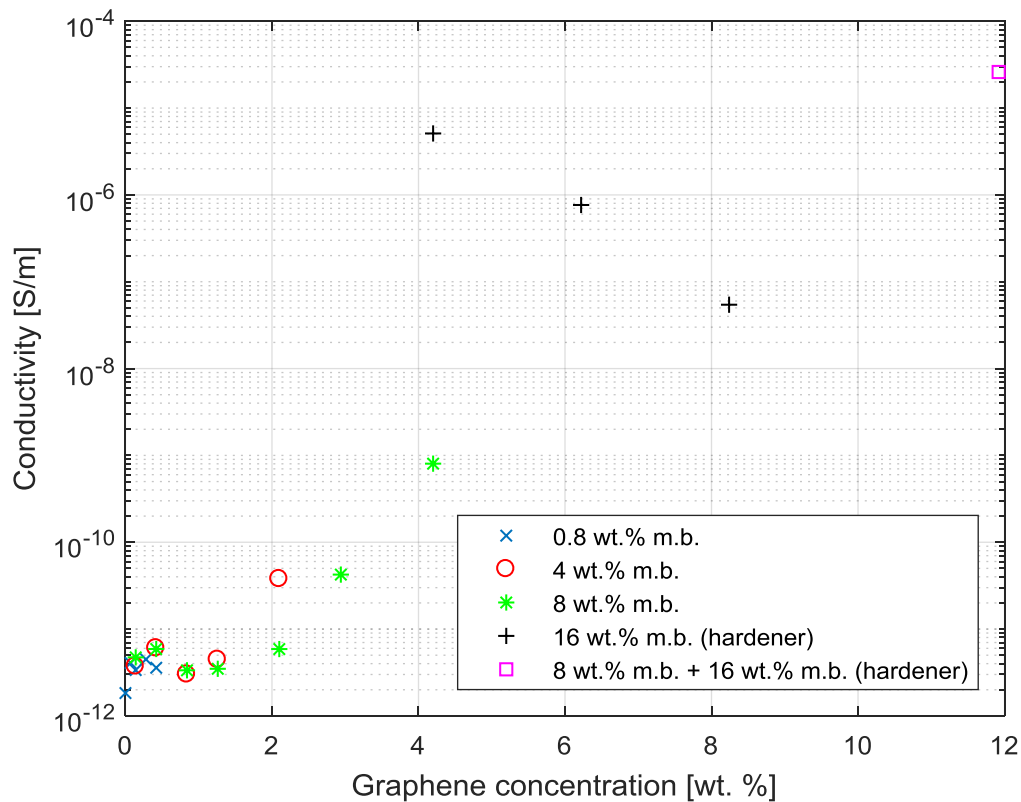


Figure 6.2 Measured electrical conductivity as a function of graphene concentration for the different samples.

7 Terahertz measurements

Terahertz transmission measurements were carried out in ambient air using the set-up in Figure 3.1. The absorption coefficient of the samples was extracted using Eq. (3) and the real part of the refractive index was determined using Eq. (2). Both quantities depend on frequency, but the results are reported here at a frequency at 0.3 THz, because this was the highest frequency which gave a good signal for all samples, and because no significant spectral features were observed in the data. Figure 7.1 shows the measured absorption coefficient for the different samples. It is clear from the figure that the absorption coefficient increases with increasing graphene concentration. Note that one of the measurements at 0 wt. % graphene concentration (i.e. neat epoxy) shows negative absorption, but this is unphysical and represents the typical measurement uncertainty.

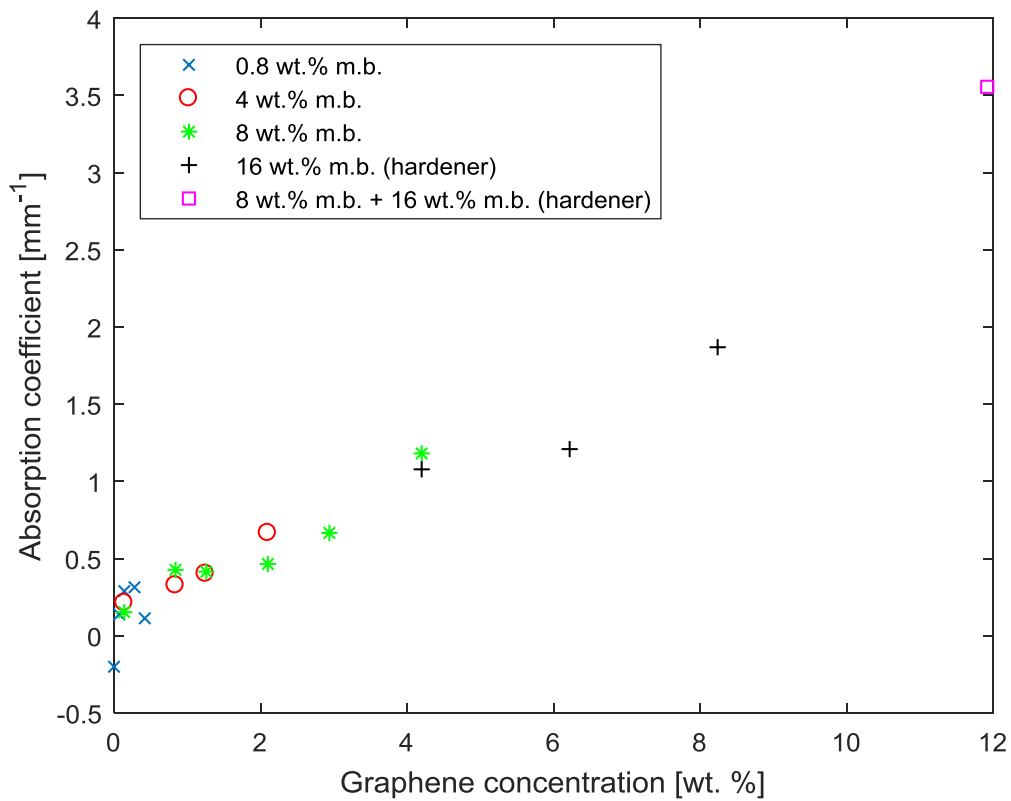


Figure 7.1 Measured absorption coefficient at a frequency of 0.3 THz as a function of graphene concentration for the different samples. Fresnel reflection at the sample interfaces is corrected for.

The real part of the measured refractive index at 0.3 THz is shown in Figure 7.2. It is apparent from the figure that the real part of the refractive index also increases with increasing graphene concentration. This manifested itself as an increase in the propagation delay of the THz pulses through the samples as the graphene concentration increased.

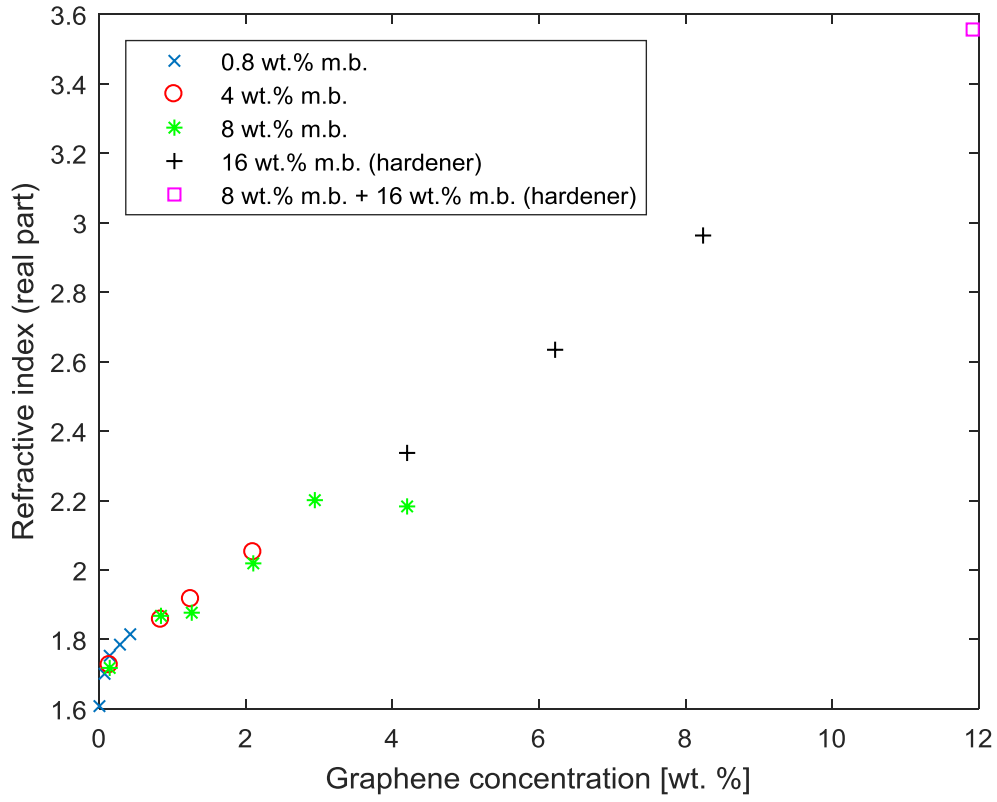


Figure 7.2 Measured real part of the refractive index at a frequency of 0.3 THz as a function of graphene concentration for the different samples.

8 Discussion

One may ask if the measured absorption coefficient at 0.3 THz can be explained by the electrical conductivity. According to one of Maxwell's equations:

$$\nabla \times \vec{H} = -i\omega\epsilon_0 \left(\epsilon + \frac{i\sigma}{\omega\epsilon_0} \right) \vec{E}, \quad (7)$$

one can define an effective permittivity

$$\epsilon_{eff} = \epsilon + \frac{i\sigma}{\omega\epsilon_0}. \quad (8)$$

The relative permittivity and the refractive index are related according to $n_{\text{eff}} = \epsilon_{\text{eff}}^{1/2}$. We observe that the electrical conductivity shows up as an effective loss term (imaginary part of the effective permittivity). By assuming $\sigma = 10^{-5}$ S/m, $\omega = 2\pi \cdot 0.3$ THz, and $\epsilon = 1.7^2$, we obtain $\epsilon_{\text{eff}} = 2.89 + 6 \cdot 10^{-7}i$, which corresponds to an absorption coefficient of about 10^{-5} /mm. This is several orders of magnitude lower than the measured absorption coefficient. We can thus conclude that the electrical conductivity of the samples has a negligible contribution to the absorption coefficient.

9 Conclusions

In conclusion, we have fabricated epoxy samples with various concentrations of dispersed graphene powder. The electrical conductivity of the samples was measured. In addition, terahertz transmission spectroscopy was used to retrieve the dielectric parameters of the samples. It was found that the electrical conductivity increased by several orders of magnitude with increasing graphene concentration, but even for the highest graphene concentration of 12 wt. %, the electrical conductivity was comparably low. Also, the measured electrical conductivity was several orders of magnitude too low to explain the measured absorption coefficient of the samples, which increased with increasing graphene concentration.

The typical military application related to this study, is the use of graphene/epoxy composites as a radar absorber. However, very important military applications of epoxy are composites, adhesives and coatings. Graphene/epoxy systems with improved properties could have a profound impact on materials in, for example, aerospace applications. Similar materials are already used as coatings for de-icing. A similar procedure for preparing graphene/epoxy composites, as applied in this case, will also be relevant for other application areas.

10 Future work

The next step would be to investigate other graphene powders than the one employed in this study. The graphene employed here has a multi-layered structure, and it would be of interest to investigate whether graphene consisting of only few layers exhibits the same behavior. CealTech has prepared master batches of reduced graphene oxide (rGO) that are currently available.

Future work could also investigate other properties (such as mechanical and ballistic) of the graphene/epoxy materials used in this study.

11 Acknowledgement

We are greatly indebted to Anh Hoang Dam, Johann Mastin and Michel Eid at CealTech AS for dispersing the graphene powder into the epoxy and the hardener. We would also like to thank the leader of “Kompetansegruppe Materialteknologi” at FFI, Tom Thorvaldsen, for providing the financial support to this activity.

Appendix

A.1 List of graphene/epoxy samples

Table 11.1 Overview of the compositions of the graphene/epoxy samples. The samples were disks with ~41 mm diameter and 1-2 mm thickness.

Sample number	Sample ID	Master batch	Graphene content in master batch (wt. %)	Graphene content in sample (wt. %)
1	neat-1	n/a	0.0	0.00
2	S3-0.42-1	S3	0.8	0.42
3	S3-0.28-1	S3	0.8	0.28
4	S3-0.14-1	S3	0.8	0.14
5	S3-0.07-1	S3	0.8	0.07
6	S4-0.42-1	S4	4.0	0.42
7	S5-0.42-1	S5	8.0	0.42
8	S4-0.14-1	S4	4.0	0.14
9	S4-0.84-1	S4	4.0	0.84
10	S4-1.26-1	S4	4.0	1.26
11	S4-2.10-1	S4	4.0	2.10
12	S5-0.14-1	S5	8.0	0.14
13	S5-0.84-1	S5	8.0	0.84
14	S5-1.26-1	S5	8.0	1.26
15	S5-2.10-1	S5	8.0	2.10
16	S5-2.94-1	S5	8.0	2.94
17	S5-4.20-1	S5	8.0	4.20
18	S8-4.20-1	S8	16.0	4.20
19	S8-6.22-1	S8	16.0	6.22
20	S8-8.24-1	S8	16.0	8.24
21	S5/S8-11.92-1	S5/S8	8.0/16.0	11.92

Master batch S3, S4 and S5 were graphene in epoxy, while master batch S8 was graphene in hardener.

A.2 Specifications of the commercial graphene powder used in the samples

- Average thickness: 10-20 nm
- Average transverse dimension: 5 μm
- Specific surface area: $\geq 15 \text{ m}^2/\text{g}$
- True density: $\leq 2.20 \text{ g/cm}^3$
- Solids: $\geq 98.80\%$
- Moisture: $\leq 1.20\%$
- Carbon content: $\geq 95.00\%$
- Oxygen content: $\leq 4.00\%$
- Hydrogen content: $\leq 1.00\%$
- Nitrogen content: $\leq 0.20\%$
- Ash content: $\leq 2.50\%$

References

- [1] M. Tonouchi, "Cutting-edge terahertz technology," *Nature Photonics.*, vol. **1**, pp. 97–105, Feb. 2007.
- [2] T. R. Sjørgård, A. D. van Rheenen, and M. W. Haakestad, "Terahertz imaging of composite materials in reflection and transmission mode with a time-domain spectroscopy system," in SPIE Photonics West, San Francisco, USA, Feb. 2016, paper no. 9747-39
- [3] F. Ellrich, T. Weinland, D. Molter, J. Jonuscheit, and R. Beigang, "Compact fiber-coupled terahertz spectroscopy system pumped at 800 nm wavelength," *Review of Scientific Instruments*, vol. **82**, no. 5, p. 053102, 2011.
- [4] Matthew J. Allen, Vincent C. Tung, and Richard B. Kaner, "Honeycomb Carbon: A Review of Graphene", *Chem. Rev.* 2010, **110**, 132–145.
- [5] Jiajie Liang, Yan Wang, Yi Huang, Yanfeng Ma, Zunfeng Liu, Jinming Cai, Chendong Zhang, Hongjun Gao, and Yongsheng Chen, "Electromagnetic interference shielding of graphene/epoxy composites", *CARBON* **47** (2009) 922 –925.
- [6] S. Bellucci, F. Micciulla, V. M. Levin, Yu. S. Petronyuk, L. A. Chernozatonskii, P. P. Kuzhir, A. G. Paddubskaya, J. Macutkevicius, M. A. Pletnev, V. Fierro, and A. Celzard, "Microstructure, elastic and electromagnetic properties of epoxy-graphite composites", *AIP Advances* **5**, 067137 (2015).
- [7] Jiacheng Wei, Thuc Vo and Fawad Inam, "Epoxy/graphene nanocomposites – processing and properties: a review", *RSC Adv.*, 2015, **5**, 73510.
- [8] Ahmed S. Wajid, H. S. Tanvir Ahmed, Sriya Das, Fahmida Irin, Alan F. Jankowski, Micah J. Green, "High-Performance Pristine Graphene/Epoxy Composites With Enhanced Mechanical and Electrical Properties", *Macromol. Mater. Eng.* **298**, 339–347 (2013).
- [9] "Graphene – Potential platform applications", Technology Watch, Science and Technology Organization (STO), NATO, AVT-TW-008, 2017

About FFI

The Norwegian Defence Research Establishment (FFI) was founded 11th of April 1946. It is organised as an administrative agency subordinate to the Ministry of Defence.

FFI's MISSION

FFI is the prime institution responsible for defence related research in Norway. Its principal mission is to carry out research and development to meet the requirements of the Armed Forces. FFI has the role of chief adviser to the political and military leadership. In particular, the institute shall focus on aspects of the development in science and technology that can influence our security policy or defence planning.

FFI's VISION

FFI turns knowledge and ideas into an efficient defence.

FFI's CHARACTERISTICS

Creative, daring, broad-minded and responsible.

Om FFI

Forsvarets forskningsinstitutt ble etablert 11. april 1946. Instituttet er organisert som et forvaltningsorgan med særskilte fullmakter underlagt Forsvarsdepartementet.

FFIs FORMÅL

Forsvarets forskningsinstitutt er Forsvarets sentrale forskningsinstitusjon og har som formål å drive forskning og utvikling for Forsvarets behov. Videre er FFI rådgiver overfor Forsvarets strategiske ledelse. Spesielt skal instituttet følge opp trekk ved vitenskapelig og militærteknisk utvikling som kan påvirke forutsetningene for sikkerhetspolitikken eller forsvarsplanleggingen.

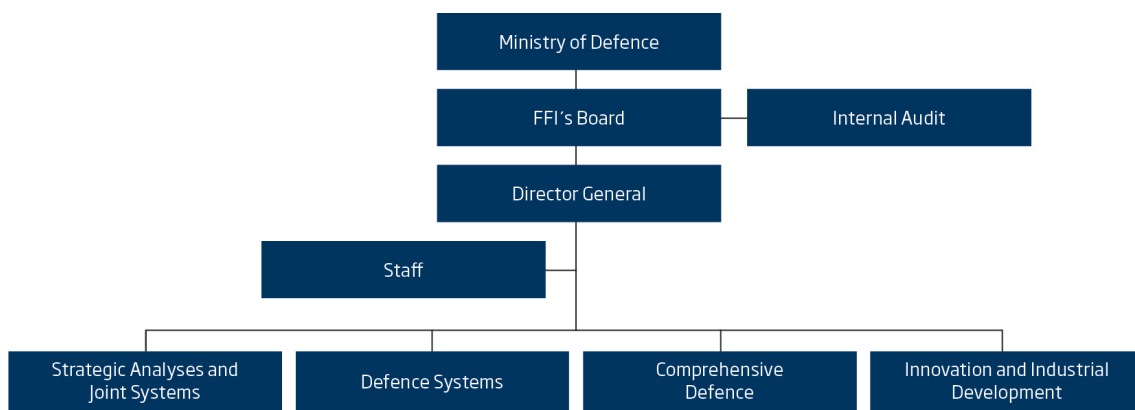
FFIs VISJON

FFI gjør kunnskap og ideer til et effektivt forsvar.

FFIs VERDIER

Skapende, drivende, vidsynt og ansvarlig.

FFI's organisation



Forsvarets forskningsinstitutt
Postboks 25
2027 Kjeller

Besøksadresse:
Instituttveien 20
2007 Kjeller

Telefon: 63 80 70 00
Telefaks: 63 80 71 15
Epost: ffi@ffi.no

Norwegian Defence Research Establishment (FFI)
P.O. Box 25
NO-2027 Kjeller

Office address:
Instituttveien 20
N-2007 Kjeller

Telephone: +47 63 80 70 00
Telefax: +47 63 80 71 15
Email: ffi@ffi.no